
THE CLUSTER DEPTH TESTS: TOWARD POINT-WISE STRONG CONTROL OF THE FAMILY-WISE ERROR RATE IN MASSIVELY UNIVARIATE TESTS WITH APPLICATION TO M/EEG

Jaromil Frossard

Faculté de Psychologie et des Sciences de l'Éducation
University of Geneva
Geneva, Switzerland
jaromil.frossard@unige.ch

Olivier Renaud

Faculté de Psychologie et des Sciences de l'Éducation
University of Geneva
Geneva, Switzerland
olivier.renaud@unige.ch

October 14, 2021

ABSTRACT

The cluster mass test has been widely used for massively univariate tests in M/EEG, fMRI and, recently, pupillometry analysis. It is a powerful method for detecting effects while controlling weakly the family-wise error rate (FWER), although its correct interpretation can only be performed at the cluster level without any point-wise conclusion. It implies that the discoveries of a cluster mass test cannot be precisely localized in time or in space. We propose a new multiple comparison procedure, the cluster depth tests, that both controls the FWER while allowing an interpretation at the time point level. The simulation study shows that the cluster depth tests achieve large power and guarantee the FWER even in the presence of physiologically plausible effects. By having an interpretation at the time point/voxel level, the cluster depth tests make it possible to take full advantage of the high temporal resolution of EEG recording to precisely time the appearance of an effect.

Keywords Multiple Comparisons Procedure · Permutation Test · Neurosciences · TFCE

1 Introduction

Bullmore et al., 1999 introduced the cluster mass test for fMRI data (functional magnetic resonance imagery) and Maris and Oostenveld, 2007 adapted it for EEG (electroencephalography) data. It has since been adopted for pupillometry analysis (Hochmann & Papeo, 2014). In all these cases, the statistical problem is the same: we want to test the difference between two or several conditions on signals, usually originated from measures on participants of an experiment. It can be one-dimensional signals – in time – for one EEG channel or pupillometry, or multidimensional signals – in space and time – in fMRI or multichannel EEG. We are interested in assessing the differences between experimental conditions without any prior information on the location or on the timing of the potential true effects. In addition, the number of locations where there might be a difference is usually large (e.g., 600 time points \times 128 channels in multichannel EEG), and each corresponds to one hypothesis. From the nature of the data, the true effects are usually adjacent, in space and/or in time. This setting is often called “massively univariate tests” (Luo & Nichols, 2003) as it involves many tests using the same design. Statistically, it is part of the multiple comparisons problem.

1.1 Classification of Tests and Error Rates

In the multiple comparisons problem, it is useful to classify the result of a procedure on m hypotheses in a 2×2 table (Table 1) similarly to Benjamini and Hochberg, 1995. Let R be the number of hypotheses called significant by the procedure, comprising S correctly rejected hypotheses (also called true discoveries or true positives) and V falsely rejected hypotheses (also called false positives, false discoveries or type I errors). Among the non-significant tests, U are correctly non-rejected (or true negatives) hypotheses and T are false negatives (or type II errors) hypotheses. Based on Table 1, the first characterization of a multiple comparisons procedure is its family-wise error rate (FWER), which is the probability of making at least one false positive, i.e., $\text{Prob}(V > 0)$.

A multiple comparisons procedure is said to control weakly the FWER if it guarantees that $\text{Prob}(V > 0 | m = m_0) = \alpha_{FWER}$, where the probability is computed under the “full null” hypothesis, e.g., under the situation where all null hypotheses are true. Otherwise, if merely one of the m hypotheses is under the alternative, the procedure does not guarantee a control of the false positive for the remaining $m - 1$ hypotheses. If a procedure controls only weakly the FWER, true discoveries are often coupled with false positives.

By contrast, a multiple comparisons procedure is said to control strongly the FWER if it guarantees that $\text{Prob}(V > 0) = \alpha_{FWER}$ for all possible combinations of true null and true alternative hypotheses (Dunn, 1958). The strong control of the FWER implies a fixed maximal error rate for any configurations in the underlying process. It provides therefore an ideal control, as we do not know the suitable configuration. The well-known Bonferroni (Dunn, 1958) or Holm (Holm, 1979) corrections both control strongly the FWER. However, to achieve this goal with a universal simple procedure, they use such loose inequalities that for massive correlated tests the actual FWER is much lower than the target value of α_{FWER} and the statistical power is disastrous (Groppe et al., 2011). In the re-sampling setting, the max- T and min- p procedures from Westfall and Young, 1993 or the method proposed by Troendle, 1995 control strongly the FWER as well. These methods benefit from the correlation between the tests that is preserved with permutation tests and adapt the correction to achieve a FWER at the target value of α_{FWER} . In massively univariate tests, these procedures are therefore far more powerful than Bonferroni and Holm.

Table 1: Classification of the result of a multiple testing procedure, as in Benjamini and Hochberg, 1995. We are testing m hypotheses, of which m_0 are under the null. We declare R hypotheses significant, including S correctly rejected and V false positives. Among the non-significant tests, U are correctly non-rejected and T are false negatives.

	non-significant	significant	
True H_0	U	V	m_0
True H_A	T	S	$m - m_0$
	$m - R$	R	m

Although these procedures factor in the correlation between tests, they do not take advantage of the specific topology of massively univariate tests. In that setting, the cluster mass test (Bullmore et al., 1999; Maris & Oostenveld, 2007) aggregates the univariate tests based on spatial or temporal adjacency, which proves to drastically increase the statistical power. It should be noted that this procedure controls only weakly the FWER. It is implemented in MNE (Gramfort et al., 2014), EEGLAB (Delorme & Makeig, 2004) or permuco (Frossard & Renaud, 2018) and is also based on permutation tests.

The cluster mass test procedure is fully described in Section 3. Its output declares zero, one or several significant cluster(s). A cluster is a set of adjacent time points that are aggregated to increase the power of the test. However, the interpretation of a significant cluster is not straightforward, and we cannot interpret each time point separately (point-wise interpretation). Formally, the cluster mass test only allows us to declare that we take an α_{FWER} risk when claiming “there is at least one alternative hypothesis within the significant cluster”. Subsequently, if we would allow ourselves to reject the null hypothesis for all time points within a significant cluster, we take a larger (and unknown) risk of a false positive than the preselected FWER target α_{FWER} . In other words, a significant cluster that contains true positives has also a large probability to include false positives as well. This is the reason, despite its many advantages, the cluster mass test cannot be used to time or to precisely localize effects (Groppe et al., 2011; Sassenhagen & Draschkow, 2019). In particular, it would be incorrect to interpret or state that the first time point of a significant cluster is the first time the conditions differ.

The TFCE (threshold-free cluster enhancement) (Smith & Nichols, 2009) is another concurring multiple comparisons procedure based on clusters that also controls weakly the FWER. It is a transformation of the statistical signals that uses the concept of cluster extent and cluster height and has the advantage of not relying on a preselected threshold parameter. Although the TFCE provides a p -value for each time point, it would be incorrect to interpret these p -values independently, and again, it would be incorrect to interpret or state that the first time point with a significant p -value is the first time the conditions differ.

The min- p and max- T approaches (Westfall & Young, 1993) are more general procedures that control strongly the FWER. They are based on permutation but do not use the information of the adjacency of the time points, unlike the cluster mass test or the TFCE. As a result, they will be less powerful than the latter, but allow us to interpret each time point significance. Finally, the method proposed by Troendle, 1995 also guarantees a strong control of the FWER. It is a stepwise procedure based on the min- p approach and has uniformly a larger power than the min- p method.

In this article, we propose a new method of multiple comparisons that combines both the idea of clusters and the algorithm of Troendle, 1995 in an effort to borrow the strength of both approaches. The aim is to provide a powerful

procedure that allows us to interpret the significance of each time point (point-wise interpretation). Using simulation, we show that our new procedure corrects the excess of false positives that would occur in a point-wise interpretation of the cluster mass test while being more powerful than the min- p or the approach from Troendle, 1995. This procedure, which we called the “cluster depth tests”, allows researchers to interpret the results in a point-wise fashion in a much more reliable way. In particular, it implies that it can be used to precisely time the appearance of an effect.

In the next section, we present the statistical models for the massively univariate tests and the cluster mass test, before explaining why the point-wise interpretation of significant clusters creates an excess of false positives when true effects are present in the signal. Then, we present our new algorithm and show how it is related to both the cluster mass test and the algorithm from Troendle, 1995. Finally, we present some simulations and an application showing the advantages and limitations of our new method.

2 Massively Univariate Tests in General Linear Model

In the simplest cases, we want to test the difference between experimental conditions on m dependent variables. These m dependent variables are distributed in time and/or in space. The present article focusses only on one-dimensional signals (e.g., one EEG channel), so the m dependent variables are the responses for the m time points. We write the models as follows:

$$Y_s = X\beta_s + \epsilon_s \quad \forall s \in \{1, \dots, m\} \tag{1}$$

where Y_s is the response variable vector for time point s , X is the design matrix shared by the m time points, β_s is the parameter vector of interests of length q and, finally, ϵ_s the error terms. We assume that each ϵ_s follows an unknown, exchangeable distribution. Importantly, ϵ_s may be correlated across the m tests. Equation 1 encompasses models for analyses like regression, t -test or one-way ANOVA. In all these models, the tests of interest can usually be viewed as testing simultaneously $q - 1$ contrasts:

$$H_{0:s} : G\beta_s = 0, \tag{2}$$

where G is a $q - 1 \times q$ contrast matrix. The F or t statistic are typical choices as the univariate test statistic for each m time point, but the procedures can accept any statistic. Let F_s be the statistic at time point s . The theory behind all multiple testing procedures is based on the (unknown) joint distribution of the statistics $[F_1 \dots F_m]^\top$. If the experiment contains more than one factor, the methods presented in Winkler et al., 2014 Kherad-Pajouh and Renaud, 2010 and Frossard and Renaud, 2018 to test any main or interaction effect can easily be extended to cover all multiple comparisons procedures presented here, including the cluster depth tests.

3 False Discoveries in the Cluster Mass Test

The cluster mass test is well described by an algorithm. First, one computes univariate statistics (e.g., t or F statistic) for each time point of the signals to produce a statistical signal (or statistical map in higher dimensions). Then, one uses a predefined threshold (τ usually set at the 95th percentile of the parametric null distribution for the univariate

statistic) to construct clusters on the statistical signals as follows. All adjacent time points whose statistics are above the threshold create together one cluster. For each cluster, the cluster mass is computed by aggregating the univariate statistics using their sum (or sum of squares)¹. The p -values are computed for each cluster by comparing its cluster mass with the cluster mass null distribution. This distribution is computed using permutation: we permuted the signals and repeated the algorithm, i.e., we compute univariate statistics on the permuted signals, create clusters using the threshold, and compute the cluster mass for each cluster. For each permuted dataset, we keep the maximal cluster mass (if multiple clusters are found). The maximal cluster mass for all permuted datasets form together the null distribution of the cluster mass (Maris & Oostenveld, 2007).

The cluster mass test should only be interpreted at the cluster level. One correct interpretation is “We take a risk of probability α_{FWER} when claiming, there is at least one true effect within a significant cluster”. This implies that we cannot use the cluster mass test to describe with high precision a cluster’s size and location (shape in higher dimension). Formally, the concept of a false positive is not well defined in the cluster mass test as we do not have the statistical decision for each time point, although the null hypotheses of Equation 2 are defined at each time point.

In order to understand how the cluster mass test may be improved to allow a point-wise testing, up until the next section we will purposefully over-interpret the results of a cluster mass test with a point-wise interpretation (i.e., all time points within a significant cluster are interpreted as individually significant). In Figure 1, we show six cases where we observed the same noise but different true effects. In the “Full null” panel, we observed one cluster (of noise) with a small cluster mass. The cluster mass test takes only a risk α_{FWER} to call a significant cluster under the full null hypothesis, so this cluster is very likely to be deemed non-significant. In the “Alone” panel, we observed a second cluster that is produced by a true effect (gray region) that is significant. In the first two cases, no false positive is perpetrated. In the “Head” panel, a single significant cluster results from the merger of two other clusters: one cluster that is formed by the region of true effect, and one cluster that appears due to noise only. Using the point-wise interpretation of the cluster mass test, all time points within this single significant cluster have the same cluster mass, which implies the same statistical decision. It produces therefore several false positives at the head of the cluster. In the “Tail” panel, the tail of the observed cluster is affected by false positives, while in the “Both” panel both the head and the tail of the cluster are affected by false positives. Finally, in the “Center” panels, we discover one significant cluster that is the aggregation of two regions of true effect linked by noise. In practice, true cases similar to the “Head”, “Tail” or “Both” panels are not uncommon. It depends on the correlation structure of the noise, but more importantly on the chosen threshold τ and on the number of “borders” of a region of true effect. Hence, the value of the statistic for the time point (under the null hypothesis) at the border of a region of true effect has a probability near 5% to be above the threshold (when the threshold is set at the 95% of the null distribution of the parametric statistic). In this case, the observed cluster contains both time points under the null and alternative hypotheses. The above probability increases as a true effect has two borders for a one-dimensional signal and even more in higher dimensions. When the power of the test is large, more than 5% of significant clusters produced by regions of true effect contains at least one false positive². This is a lower bound that suffers greatly from the “curse of dimensionality” as this probability depends on the number of time points at the border of a region of true effect.

¹The length of the cluster can also be used (and can be viewed as a function of the statistics).

²This is an excess of false positives, as, even when some hypotheses are under the alternative, there might be significant clusters that are fully composed of null hypotheses. It would be less than 5% as we assume a true effect ($m_0 < m$).

This excess of false positives comes from the aggregation of statistics within the clusters. All time points of a cluster are associated to the same cluster mass: at the border of a region of true effect, some time points under the null hypothesis might “benefit” from the contribution of a true effect as they will all share the same cluster mass. The aim of the cluster depth tests is to take into account this excess of false positives at the head and tail of clusters. They re-use the concept of clusters created by a threshold while dropping the concept of cluster mass to reach point-wise tests within the clusters.

4 Point-Wise Significance within the Clusters: the Cluster Depth Tests

The cluster mass test is general to cases where hypotheses are distributed in time and/or in space. It only needs that some suitable adjacency between points can be defined. In this article, we restricted ourselves to one-dimensional signals as we rely on the concept of cluster depth. The cluster depth describes the position of a time point relative to the cluster’s first or last time point. Each time point within a cluster is therefore associated with two cluster depths, one from the cluster’s head and one from its tail.

If the time point s^* is the first time point of an observed cluster, or at the first cluster depth, the “classical approach” to testing its corresponding hypothesis would be to compare the observed statistic at time point s^* to the null distribution at that specific time point s^* , while taking into account that m tests are carried out (one for each time point). In that procedure, the time point s^* is relative to the start of the signal. Instead, we propose to compare the statistic at time point s^* relatively to its position within the cluster. In that case, it would be the first cluster depth (as we assumed that s^* corresponds to the first time point of an observed cluster). We produce a test for the first cluster depth as follows. First, we compute the statistic of interest for each time point of the signals; then, using the predefined threshold τ , we create clusters. The first cluster depth statistic (from the head) is the statistic of the first time point within the cluster (from its head). We produce a p -value for the first cluster depth by comparing its observed statistic with its distribution under the null hypothesis. This distribution of the first cluster depth is computed by permutation: for each permuted dataset, we compute the univariate statistics at each time point; then, using the threshold τ , we create clusters and keep the maximal values at the first cluster depth (if several clusters are created). For a given permutation, if there is no cluster, this value is set to 0. These maximal values create together the null distribution by permutation of the first cluster depth. Algorithm 1 describes this procedure, which provides a p -value for each time point associated to the first cluster depth. The distribution by permutation of the first cluster depth is interpreted as the distribution of the first value of the clusters given (1) no difference between conditions, (2) signals of length m and with the same correlation structure, and (3) clusters created using a threshold τ . Observing a large value of the statistic of first cluster depth indicates an uncommon observation under the null hypothesis for this first value. So, we would take an α risk rejecting the null hypothesis for the test associated to the first cluster depth when its p -value is inferior to α .

Note that Algorithm 1 can be viewed as a special case of the cluster mass test. Indeed, the cluster mass test uses a function to aggregate the individual statistics into a cluster mass statistic. It is usually the sum or the sum of squares of the statistics of all time points within the cluster. However, defining this function as a weighted sum, with a weight of 1 for the first time point of the cluster and a weight of 0 otherwise, gives the same procedure as Algorithm 1.

The next step is to generalize Algorithm 1 to all cluster depths and is described in Algorithm 2. We propose, for each j th cluster depth $j \in \{1, \dots, J\}$, where J is the length of the cluster, to compare the observed statistic at the j th cluster depth to its distribution under the null hypothesis. The null distribution of the j th cluster depth is computed by

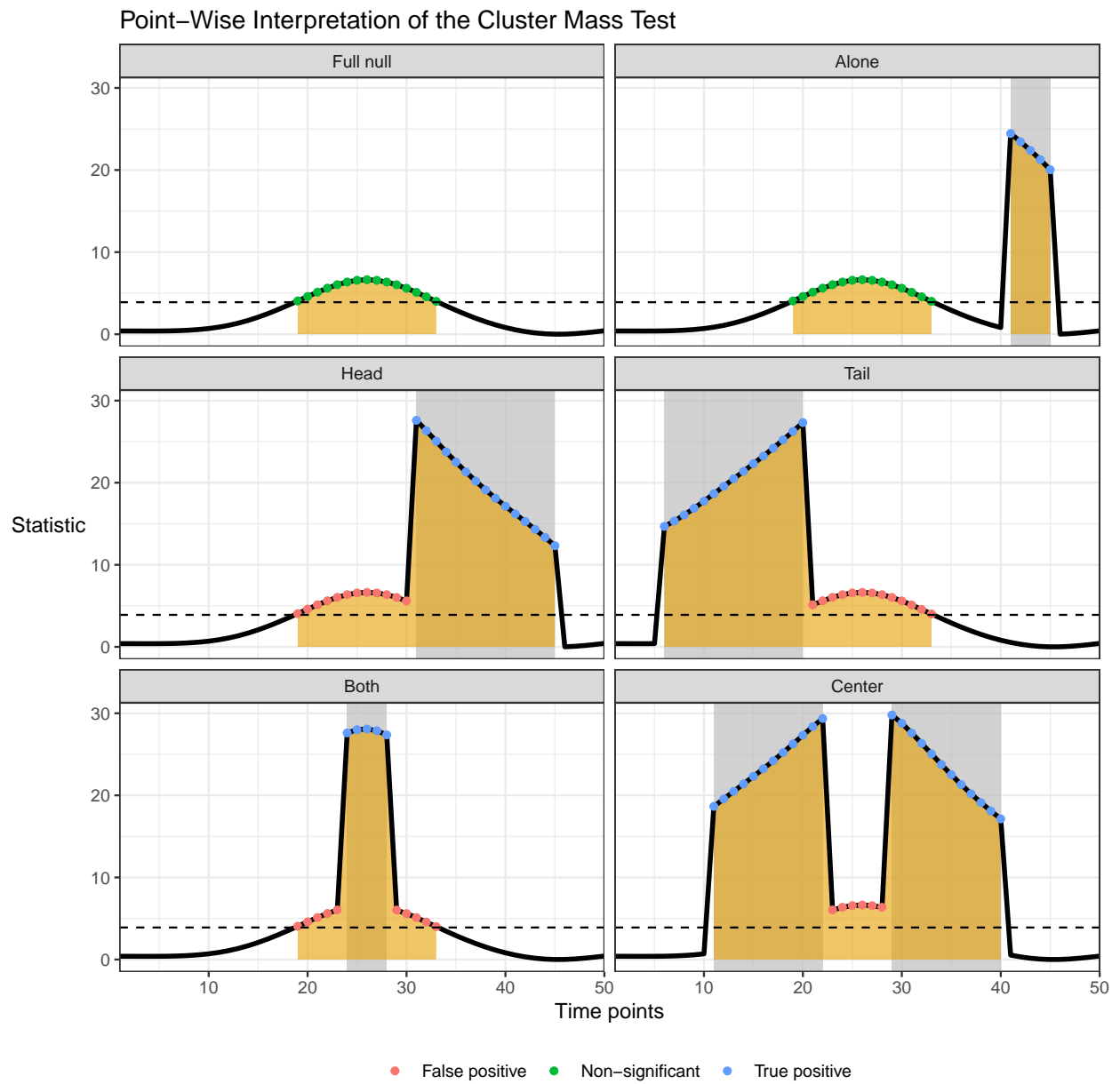


Figure 1: Six cases where regions of true effects (gray area) combine with a cluster created by noise only. The gray area indicates the presence of a region of true effect, and the orange area indicates clusters created using the predefined threshold (dashed line). In the four panels “Head”, “Tail”, “Both” and “Center”, the point-wise interpretation of the cluster mass test leads to false positives as some null hypotheses will be part of clusters driven by a true effect.

permutation where, for each permutation, we use the threshold to compute clusters and we retain the statistic at the j th cluster depth. For each permutation, if there are multiple clusters, we keep the maximal statistic of the j th cluster depth, and if no cluster is found or the maximal length of the clusters is below j , then the value is set to 0. Algorithm 2 is illustrated in Figure 2 using a simple example. Algorithm 2 produces a univariate test for each cluster depth of the observed clusters of size J . These tests are highly correlated due to the adjacency of the depths, and the permutation procedure captures correctly their full multivariate distribution. As it corresponds to J distinct tests, it would inflate the FWER to directly interpret the resulting J p -values. An additional step is therefore needed, where the FWER among these J tests is controlled using the procedure of Troendle, 1995. This method has proven to be powerful when comparing a reasonable number of tests and hence is a good candidate to control the FWER among the J cluster depth tests while maintaining a high power. Its implementation is described in the second part of Algorithm 2.

Using Algorithm 2 and computing the cluster depth from the head of the cluster only takes into account the false positives that may occur at this head (Figure 1, panel “Head”). It already improves the interpretation of significant time points. If we observed a significant effect from time points 50 to 70 using the cluster depth tests (from the head), we take an α_{FWER} risk when claiming that “there is a true difference that begins no later than time point 50” . However, we take a risk larger than α_{FWER} if we claim that the effect lasts at least to time point 70. Due to the low power at the extremities of effects, note that the difference between experimental conditions may begin sooner than 50 (or after 70), but it would imply merely a false negative or negatives.

Using Algorithm 2 while counting the depth from the cluster head does not provide any correction for the false positives that may appear at the cluster tail (Figure 1, panel “Tail”). However, by symmetry, we can apply Algorithm 2 while counting the depth from the cluster tail (or by reversing the time). Using the cluster depth from both the head and the tail produces two p -values for each time point within a cluster. To protect the FWER, we keep the largest of the two to evaluate the significance of each time point, as described in Algorithm 3. The largest will typically be the head one for the cluster’s starting point and the tail one for the ending point, but the algorithm protects automatically any case.

Algorithm 1: Inference for the first cluster depth from the head.

Result: K p -values associated to the K time points for the first cluster depth (of the K observed clusters).

Compute the univariate statistics for the m tests for the original data and all $n!$ permutations. It corresponds to $n!$ statistical signals $\tilde{\mathcal{F}}_{0:[i]}$ of length m that are stored in a $n! \times m$ matrix $\tilde{\mathcal{F}}_0$.

for each $i \in \{1, \dots, n!\}$ **do**

Using the threshold τ , compute K^* clusters on the permuted signal $\tilde{\mathcal{F}}_{0:[i]}$ as sets of adjacent time points whose statistics are above the threshold.

If $K^* = 1$, return the statistic of the first cluster depth.

If $K^* > 1$, return the maximal statistic of the first cluster depth over the K^* clusters.

If $K^* = 0$, return 0.

end

The $n!$ returned values constitute the null distribution of the first cluster depth ($D_{\text{depth: } 1}$) statistic.

Compare ($D_{\text{depth: } 1}$) to the observed statistics at the first cluster depth of the K observed clusters to produce K p -values.

Algorithm 2: Inference for all cluster depths $1, \dots, J$ from the head

Result: p -values associated to all time points within the K observed clusters.

Compute the univariate statistics for the m tests for the original data and all $n!$ permutations. It corresponds to $n!$ statistical signals $\tilde{\mathcal{F}}_{0:[j]}$ of length m that are stored in a $n! \times m$ matrix $\tilde{\mathcal{F}}_0$.

Using the threshold τ , define K clusters on the observed statistical signal as the sets of adjacent time points whose statistics are above the threshold. The length of the clusters $k = 1, \dots, K$ is J_k , and let $J = \max_k(J_k)$.

for each j th cluster depth in $1, \dots, J$ **do**

 Define $D_{\text{depth}:j}$ as the null distribution of the statistic at the j cluster depth as follows:

for each $i \in \{1, \dots, n!\}$ **do**

 Using the threshold τ , compute K^* clusters on the signal $\tilde{\mathcal{F}}_{0:[j]}$ as sets of adjacent time points whose statistics are above the threshold.

 If $K^* = 0$ or if the maximal length of the K^* clusters is $< j$, return 0 for this permutation.

 If $K^* = 1$, return the statistic at the j th cluster depth

 If $K^* > 1$, return the maximal statistic at the j th cluster depth over the clusters whose length is $\geq j$.

end

 The $n!$ returned values constitute the null distribution of the statistic at the j th cluster depth : $D_{\text{depth}:j}$ statistic.

end

Keeping the same order of the permutations, the $n!$ vectors of dimension J constitute the multivariate null distribution of the J cluster depths. Store these values in a $n! \times J$ matrix $[D_{\text{depth}:1}, \dots, D_{\text{depth}:J}]$.

Compare this multivariate distribution to the observed statistics of the K clusters in order to produce $\sum_k J_k$ p -values, which correspond to one p -value for each time point within the K clusters, as follows:

for each $k = \{1, \dots, K\}$ clusters **do**

 Compare the $J_k \leq J$ observed statistics of the cluster k to the multivariate null distribution

$[D_{\text{depth}:1} \dots D_{\text{depth}:J_k}]$ using the algorithm proposed by Troendle, 1995 to produce J_k corrected p -values for each time point within cluster k .

end

Algorithm 3: Controlling the false positives at the head and tail of the clusters.

Result: p -values associated to all cluster depths within the clusters.

Use Algorithm 2 to compute the cluster depth tests from the head , producing the p -values p_H .

Use Algorithm 2 to compute the cluster depth tests from the tail , producing the p -values p_T .

Take the element-wise maximum between p_H and p_T , producing the p -values p_B .

Return p_B .

5 Implementation Details and Limitations of the Cluster Depth Tests

Algorithm 2 has an unintended behavior at the border of the observed signal. This effect is visible in the Panel E from Figure 2: some clusters from permuted signals have statistical values around 10 at the first cluster depth. Indeed, for some permutations, the clusters are at the border of the sampling (1 or 80 in Figure 2). This means that for some permutations, the statistic at time point 1 has already a much larger value than the threshold and is still considered as a first cluster depth. However, if we could observe the statistic before time point 1, we would classify these values at a

higher cluster depth than the first one, since several previous points would probably be part of the cluster. Overall, this effect shifts upward a part of the distribution for lower cluster depths and downward for higher cluster depths. A simple way to circumvent this undesirable feature, using an argument of temporal symmetry, is to compute the cluster depth from the opposite direction when a permuted cluster is at the border, or equivalently to reverse these clusters.

Moreover, computing separately the cluster depth null distributions from both the head and the tail may complicate the algorithm. Using again an argument of temporal symmetry, another approach is to compute a common distribution for the j th cluster depth by taking the maximal values over both the j th cluster depth from the head and from the tail. This new approach is slightly more conservative but may be the first step to generalize the cluster depth tests to cases with hypotheses distributed on a raster or on a general adjacency graph.

The assumption of the cluster depth tests is the same as for the cluster mass test. As both the cluster depth tests and the cluster mass test compare statistics from different time points, under the full null hypothesis the statistical signal should be stationary. Note that this does not require that the individual signals are stationary, but if they are, this implies the stationarity of the statistical signal.

Concerning the interpretation and limitation of the proposed method, the cluster depth tests procedure do not formally control strongly the FWER as it does not guarantee, for all combinations of null and alternative hypotheses, a FWER at the nominal level. Schematically, it controls strongly the FWER in the first five cases depicted in Figure 1 but might fail in the sixth case. The FWER is guaranteed therefore when the true effects happen in regions that are far enough apart, which often corresponds to the expected physiologically plausible effects in M/EEG. Typically, the cluster depth tests procedure will not guarantee the FWER when two true effects are separated with only one time point under the null (see the simulations in Section 6). This implies that the interpretation of the cluster depth tests should not be a fully point-wise interpretation of the tests. For instance, finding significant time points from 50 to 70 with the cluster depth tests would formally allow us to declare the following at an α_{FWER} risk: “There is at least one region of true effect from time points 50 to 70, beginning no later than time point 50 and ending no earlier than 70.” However, we do not know exactly how many true region(s) there might be within the time frame. Note that the interpretation would be the same if all observed statistics from time points 50 to 70 are above the threshold (they form together one cluster), but only the time points from 50 to 55 and 65 to 70 are declared significant using the cluster depth tests. In that example, only the borders at time points 50 and 70 are controlled for false positives. Note, however, that these mistakes that make the cluster depth tests miss the strong control of the FWER will happen quite rarely: not only must two true effects be close to one another, but in conjunction all time points in-between (that are under the null) should maintain a statistic above the threshold, which by definition of the threshold occurs in less than 5% of the cases. Moreover, physiologically plausible effects always start and end slowly, which substantially increases the probability that at least one time point is below the threshold, cutting the cluster in two and decreasing the false positive rate.

6 Simulation Study: FWER and Power

We simulate signals of length $m = 400$, from two groups of 10 participants, and we test the differences between the two conditions with an F statistic and compare several multiple comparisons procedures. We change the correlation between the error terms of time points using either an independent, a Gaussian or an exponential autocovariance function (Abrahamsen, 1997). In all simulation settings, the univariate error terms follow standard normal distribution.

The Cluster Depth Tests

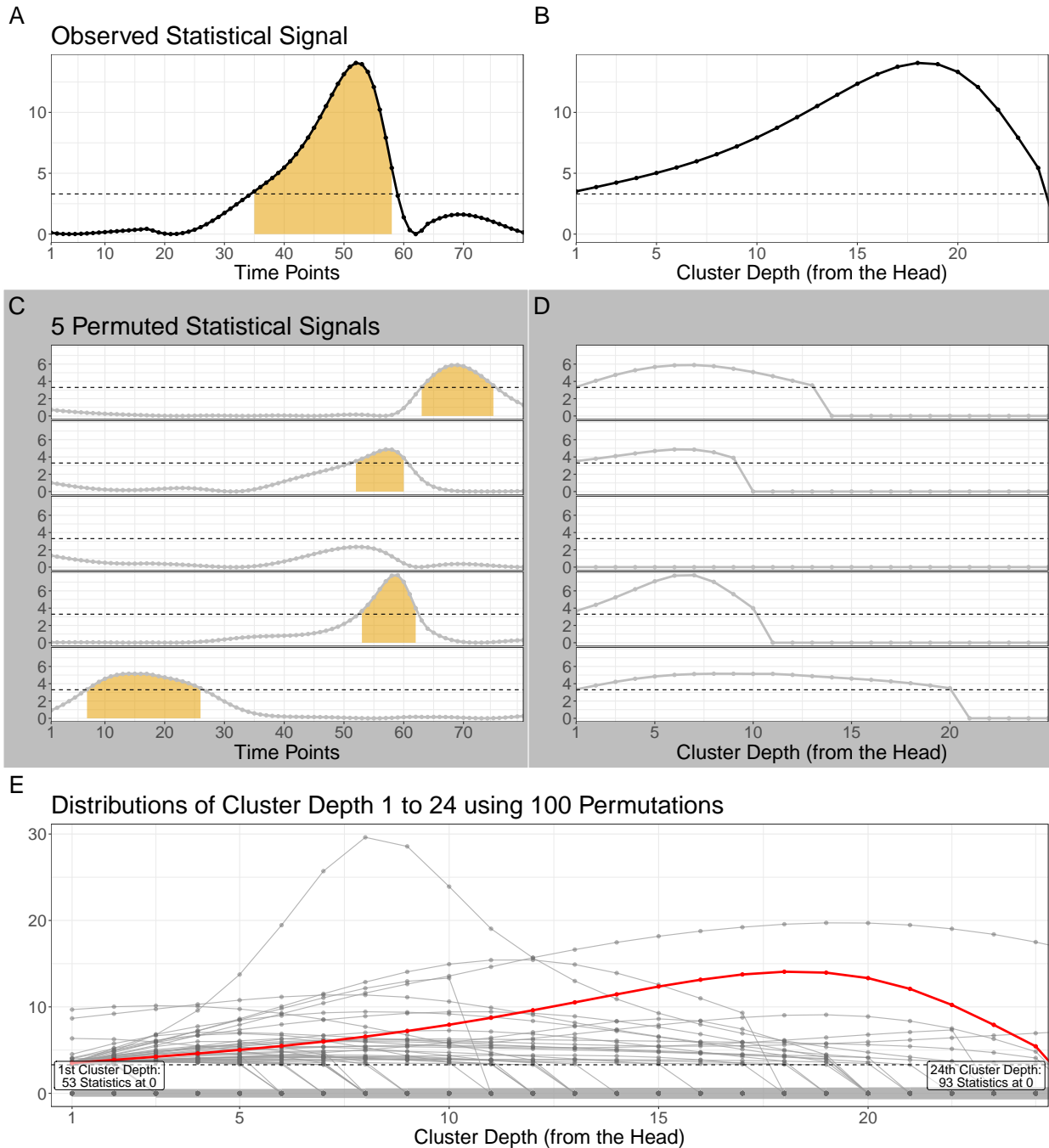


Figure 2: Cluster depth tests (from the head) as described in Algorithm 2. Panel A shows the observed statistical signal, which contains one cluster. In Panel B, we extract the cluster of length 24. Panel C shows five permuted signals. For each permuted signal, we computed clusters (orange) and re-align them according to their cluster depth (Panel D). In Panel E, for each cluster depth the observed statistic (in red) and its distribution under the null hypothesis (formed by all dots in gray) are shown. Finally, using the method from Troendle, 1995, we test individually each cluster depth while taking into account the 24 tests.

Moreover, we vary the number of regions of true effects (0, 1 or 2) and the number of time points under the alternative (1%, 10%, 20%, 40% or 60% of m). We also change the shape of these regions, including a square-shaped effect region, where the β_s are either 0 or $\beta_{max} \neq 0$, and a region with a right-angled triangular-shaped effect where the β_s 's increase linearly from 0 (at the beginning) to $\beta_{max} \neq 0$ at the end of the region of true effect. Finally, we modify the values of $\beta_{max} \in \{0.2, 0.8, 1, 1.5, 2\}$ to better understand its influence on the tests of regions under the null hypothesis (FWER) and on their power in the regions under the true effect.

We then control for multiple comparisons using the min- p approach (Westfall & Young, 1993), the procedure from (Troendle, 1995), the cluster mass test (Maris & Oostenveld, 2007) with a threshold at the 95th percentile of the statistic and the TFCE (Smith & Nichols, 2009) (with $H = 1$ and $E = 0.5$ as suggested in Pernet et al., 2015) that we compared to the cluster depth tests (with the same threshold as the cluster mass test).

We also compared two different versions of the cluster depth tests concerning the border handling method: either we ignore the effect of permuted clusters at the border ("Ignore") or we reverse the computation of the cluster depth when a permuted cluster is found at the border ("Reverse") of the time frame. We also compare the computation of the cluster depth distribution using either the two distributions from the head and from the tail separately ("Separately H-T") or a unique cluster depth distribution as the maximum of both cluster depths from head and tail ("Max H-T"), as proposed in Section 5.

All simulations are performed using the permuco package (Frossard & Renaud, 2018); the cluster depth test is currently available in the "rcpp" branch (<https://github.com/jaromilfrossard/permuco>)³. We measure the FWER as the proportion of simulations that exhibit at least one false discovery (with 95% CI using Agresti and Coull, 1998), i.e., for which at least one time point outside the true effect region is called significant. Two aspects of power are evaluated: first, the average percentage of true discovery within the region of true effect (average power), and second, the proportion of simulation where at least one time point under a region of true effect is significant (disjunctive power, Bretz et al., 2010). The min- p and Troendle, 1995 procedures and the cluster depth tests are meant to be interpreted point-wise, whereas such a point-wise interpretation of the cluster mass and TFCE procedures would represent an over-interpretation of their results, as they do not pretend point-wise interpretation of the significance, as explained in Section 3. However, for the sake of the comparison, it is of interest to see how different the point-wise interpretation of the proposed method differs from these two approaches.

The results of the FWER for all the settings described in the first paragraph and all the multiple testing procedures are shown in Figure 3 for a square-shaped effect and in Figure A.1 for a triangular-shaped effect. The different columns show the results for signals with a different proportion of time points under true effect and a different number of regions of true effect. In the last column, no time points are under the true effect, i.e., the signals are under the full null ($m_0 = m$). The color luminance represents the strength of the effect in the region(s) of true effect, but the FWER is of course computed in all time points that are outside this/these region(s).

A method that would strongly control the FWER would have bars that are always at the 5% level or lower, being conservative when it is less than 5%. Note that it would control the FWER only weakly if the bars are at the 5% level or lower only in the last column and in the "null"/lighter colored cases.

³It can be installed using the remotes package (Hester et al., 2020) with `remotes::install_github("jaromilfrossard/permuco@rcpp")`

As expected, the min- p and Troendle, 1995 multiple comparisons procedures control strongly the FWER even in the presence of one region or two distant regions of true effect (Figure 3 and Figure A.1). However, we see that they are extremely conservative with FWER often even equal to 0 when the noise is independent. This can be explained by the equivalent number of independent tests, which are much larger if the noise is independent than if it is highly correlated, as with the exponential or Gaussian autocovariance cases. This shows that these methods do not scale with an increasing number of tests and do not benefit from the temporal adjacency of the region of true effect. In the settings of Figures 3 and A.1, these simulations show that the proposed cluster depth test also controls the FWER. On the contrary, the cluster mass test does not guarantee the FWER when true effects are present, although it controls (weakly) the FWER (full null). Finally, in these simulation settings, although with a FWER sometime significantly larger than 5%, the TFCE is generally close to the FWER target, which is not theoretically guaranteed. This confirms the good property of an extend parameter $H < 1$ as suggested by Smith and Nichols, 2009 and Pernet et al., 2015.

The two aspects of the empirical power in the same settings as in the two previous figures are displayed in Figures 4 and A.5. The cluster depth tests achieve a very high power, even larger than the cluster mass test, when the region of true effect is small. The power of the cluster depth tests is also systematically higher than the TFCE power, especially when the true effects have a small effect size/signal-to-noise ratio. This is an outstanding performance since the cluster mass and TFCE do not control the FWER and therefore should not even be displayed. Using our simulation setting, and especially when the region of true effect is small, the min- p or Troendle, 1995 procedures exhibit a much lower power than the cluster depth tests.

In order to see the limit of the proposed method, we simulated data under its least favorable case. Figure 5 shows the empirical FWER when two regions of true effect are separated only by one single time point under the null. As expected, the cluster depth tests fail to keep the FWER at the 5% level and therefore do not guarantee the strong control of the FWER when several true regions are too close. Note, however, that it is never higher than 10% in this least favorable case.

Finally, Figure A.2 and Figure A.3 show different parametrizations of the cluster depth tests. We change the method to handle permuted clusters at the border of the time frame: either we reverse the computation of the cluster depth (“Reverse”) for these particular clusters, or we do not change the algorithm, ignoring the potential effect (“Ignore”). Moreover, we compute two distinct distributions of the cluster depth from the head and from the tail, (“Separately H-T”), or we compute one cluster depth distribution of the maximum over the head and tail (“Max H-T”) as described in Section 5. As expected, using a unique cluster depth distribution of the maximum (“Max H-T”) is more conservative relatively to two distributions for the head and for the tail (“Separately H-T”). However, the method to handle clusters at the border does not seem to affect the FWER in our simulation setting. We suggest using two distinct distributions (“Separately H-T”) and reversing the computation of the cluster depth for permuted cluster at the border of the time frame (“Reverse”). This parametrization is the one chosen as the default in the comparisons with other methods presented in Figures 3, A.1, 5,4 and A.5.

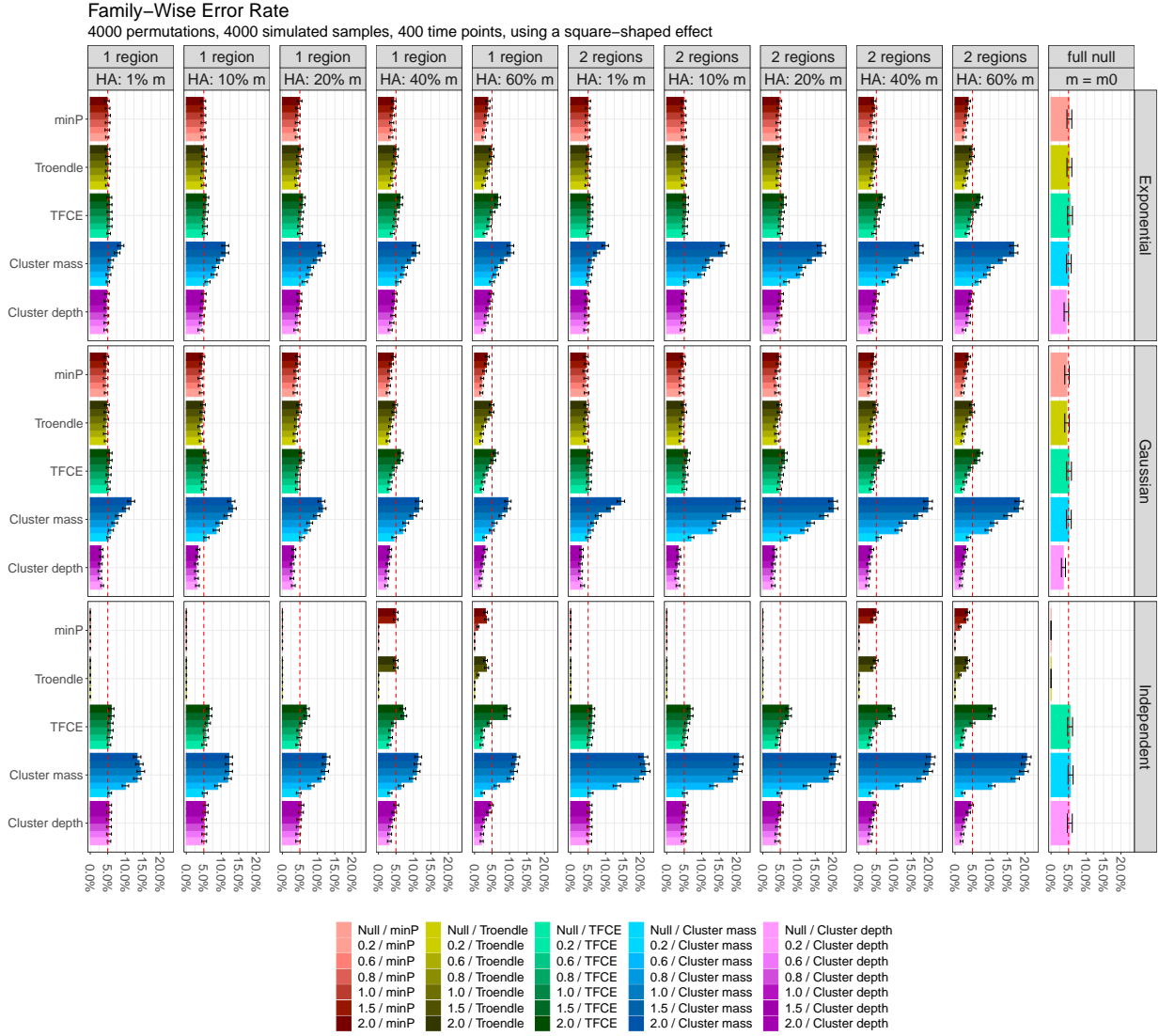


Figure 3: Empirical FWER under different numbers and lengths of true effect regions (column), different noise structures (rows) for different multiple comparisons procedures (colors) and with different effect sizes of the true effects (luminance of the colors). The FWER is computed on all time points that are under the null hypothesis. The cluster depth tests stay at the expected 5% level, whereas the min- p and Troendle, 1995 procedures can be very conservative, the cluster mass test can be very anti-conservative and the TFCE can sometimes be conservative and sometimes anti-conservative.

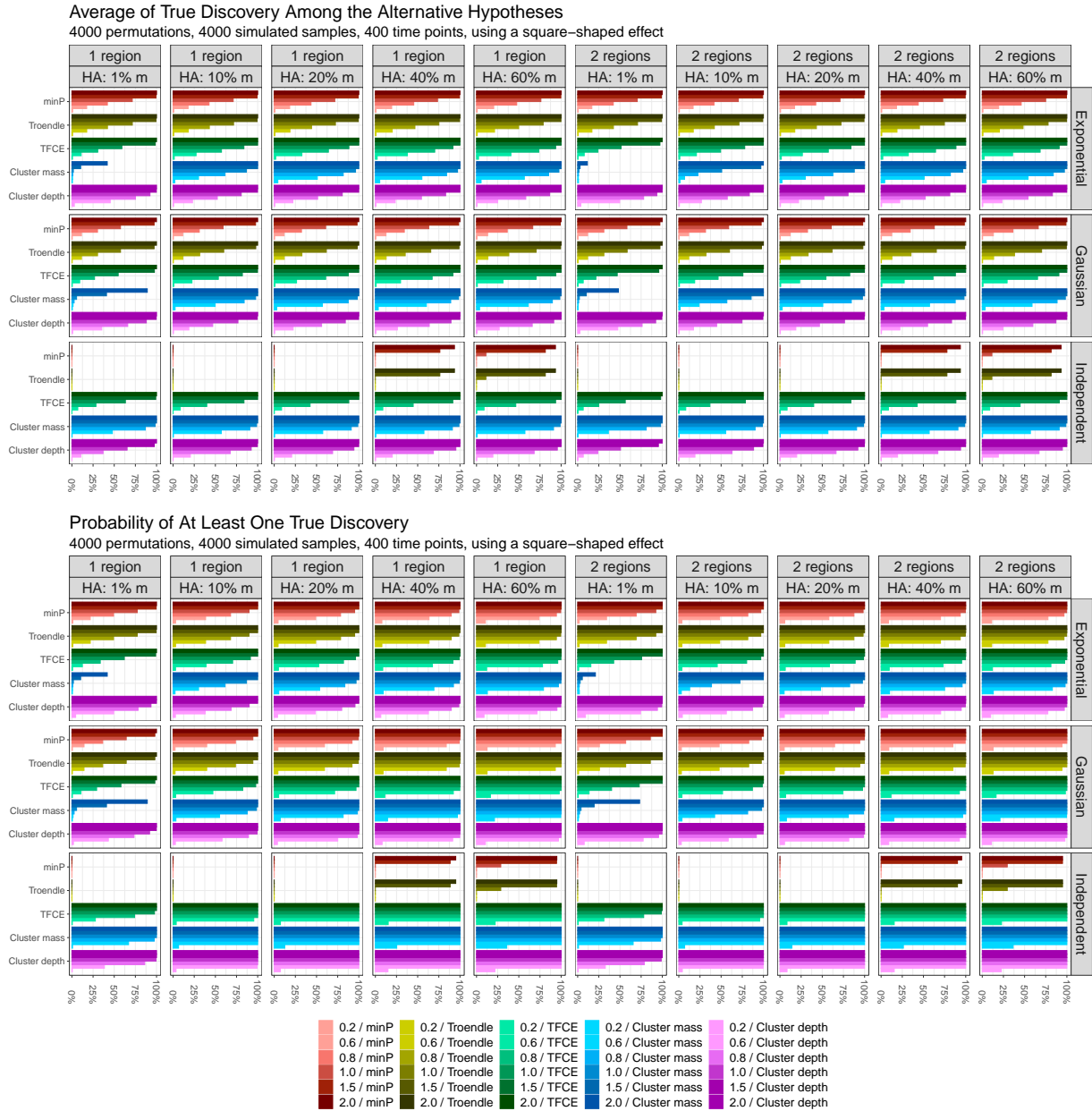


Figure 4: Average and disjunctive power for the same simulation settings presented in Figure 3. Different numbers and lengths of true effect regions are presented in columns, different noise structures in rows, the different multiple comparisons procedures in colors, and the different effect sizes of the true effects in color luminance. The cluster depth tests have an outstanding power for a procedure that controls the FWER in all these simulation settings.

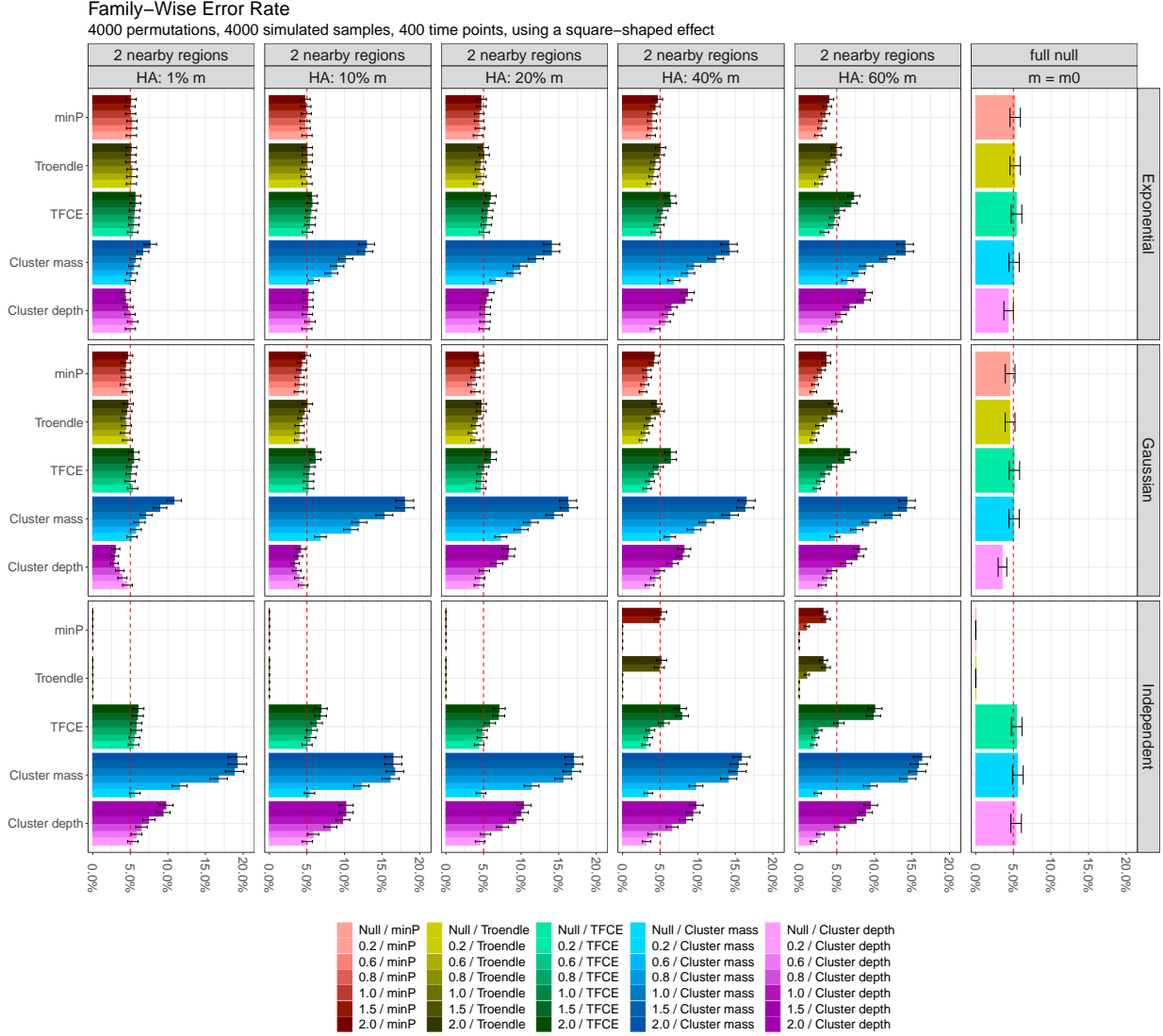


Figure 5: Empirical FWER under the least favorable case (but physiologically implausible) for the cluster depth tests. Two regions of true effect are present and are separated only by one single time point under the null. Different lengths of the true effect regions are presented in columns, different noise structures in rows, the different multiple comparisons procedures in colors, and the different effect sizes of the true effects in color luminance. As expected, the empirical FWER for the cluster depth tests grows above 5%.

7 Example of Data Analysis

Tipura et al., 2019 analyzed EEG recordings from an experiment in attention shifting. The EEG signals were recorded at 1024 Hz for 614 time points (600 ms) after the presentation of an image. Each participant is recorded in several experimental conditions, including the *visibility* of the image, either 16 ms (subliminal) or 166 ms (supraliminal); the *emotion* induced by the image, either angry or neutral; and the *direction* of the image on the screen, either on its left or

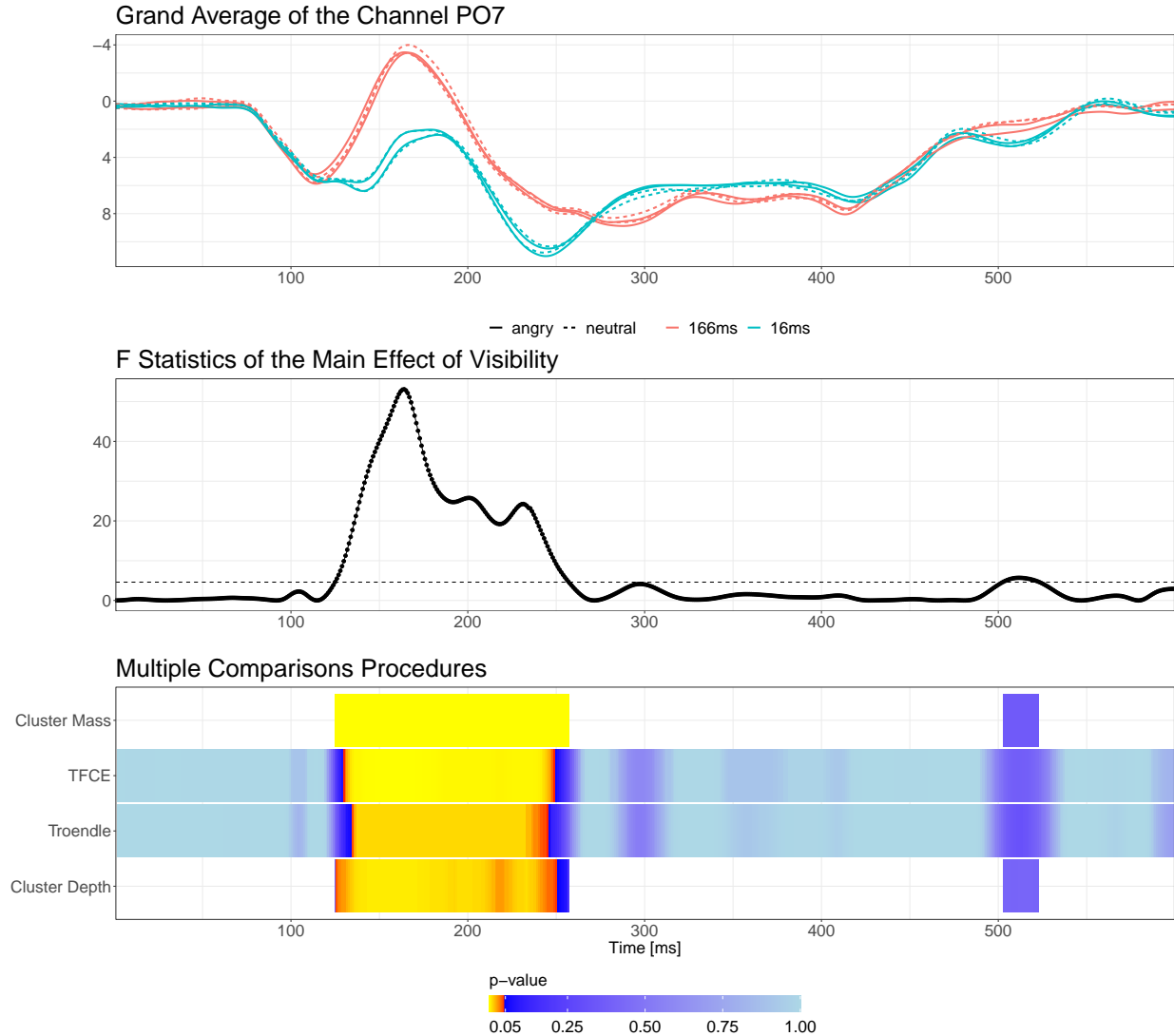


Figure 6: Grand average of the eight conditions and test of the main effect of visibility on the PO7 channel from the experiment in Tipura et al., 2019. All methods detect one cluster. However, the cluster depth tests detect the largest number of time points while taking into account the false positives at the border of the cluster.

on its right. The experimental design corresponds to a repeated measures ANOVA when averaging over the images. The permutation method from Kherad-Pajouh and Renaud, 2015 is a permutation test for the main and interaction effects in repeated measures ANOVA and can be used in combination with the multiple comparisons procedures presented in Section 1, including the cluster depth tests. Figure 6 shows the results of several multiple comparisons procedures for the main effect of the visibility of the P07 channel.

Using the cluster mass test produces a single large significant cluster that begins at the 128th measure (125ms) and ends at the 263th measure (257ms) or as soon as the statistic crosses the threshold. However, the cluster mass test does not

give evidence that the first and last time points of the significant cluster are different from noise. The significant cluster may be the combination of a cluster created by noise and a true effect as in Figure 1, Panel “Head”, “Tail” or “Both”.

When using the cluster depth tests, we found that the first cluster depth of the observed cluster is typical of one created from noise only. Therefore, we do not reject the null hypothesis for this time point. However, from time point 129 (126ms), corresponding to the second cluster depth, we observed a statistic that is uncommon for a cluster created from noise only, and we reject its null hypothesis. On the other hand, we cannot reject the null hypotheses for the seven last time points, from 257 to 263 (251ms to 257ms). It means that these seven time points are typical of the tail of clusters created from noise only. The cluster depth tests allow us to claim, with a known error rate of α_{FWER} , that the true difference between experimental conditions starts no later than 126ms and ends no earlier than 251ms. Troendle, 1995 procedure also gives a point-wise interpretation of the results. Using this method, we find a significant difference from time point 138 (135ms) to 251 (245ms). Finally, the TFCE gives a significant p -value within time points 133 (130ms) to 255 (249ms). Formally, we should not have a point-wise interpretation of the TFCE, despite its relatively good results in our simulation study.

For this dataset, the cluster depth tests seem the best multiple comparisons procedures, as they balanced the power as well as guaranteed a useful and intuitive interpretation of the results.

8 Conclusion

The cluster depth tests are a new multiple comparisons procedure for the massively univariate tests. We shows that they are closely related to the cluster mass test and to the procedure of Troendle, 1995. Using simulation, we show that it is both powerful and controls the FWER even in the presence of physiologically plausible true effects. Moreover, we show that the cluster depth tests have two main advantages in comparison to the TFCE or the cluster mass test: they allow a point-wise interpretation and can be used for the timing of effects in M/EEG.

9 Acknowledgment

Visualizations are made using the R packages, ggplot2 (Wickham, 2016), patchwork (Pedersen, 2020) and ggrepel (Slowikowski, 2020).

We thank Eda Tipura for sharing the EEG data presented in Section 7.

The simulations were performed using the “Baobab” HPC at the University of Geneva.

References

- Abrahamsen, P. (1997). *A Review of Gaussian Random Fields and Correlation Functions*. Norsk Regnesentral/Norwegian Computing Center.
- Agresti, A., & Coull, B. A. (1998). Approximate Is Better than "Exact" for Interval Estimation of Binomial Proportions. *The American Statistician*, 52(2), 119–126. <https://doi.org/10.2307/2685469>
- Benjamini, Y., & Hochberg, Y. (1995). Controlling the False Discovery Rate: A Practical and Powerful Approach to Multiple Testing. *Journal of the Royal Statistical Society B*, 57(1), 289–300.

- Bretz, F., Hothorn, T., & Westfall, P. (2010). *Multiple Comparisons Using R*. Chapman and Hall/CRC.
- Bullmore, E. T., Suckling, J., Overmeyer, S., Rabe-Hesketh, S., Taylor, E., & Brammer, M. J. (1999). Global, Voxel, and Cluster Tests, by Theory and Permutation, for a Difference between Two Groups of Structural MR Images of the Brain. *IEEE Transactions on Medical Imaging*, 18(1), 32–42. <https://doi.org/10.1109/42.750253>
- Delorme, A., & Makeig, S. (2004). EEGLAB: An Open Source Toolbox for Analysis of Single-Trial EEG Dynamics Including Independent Component Analysis. *Journal of Neuroscience Methods*, 134(1), 9–21.
- Dunn, O. J. (1958). Estimation of the Means of Dependent Variables. *The Annals of Mathematical Statistics*, 29(4), 1095–1111.
- Frossard, J., & Renaud, O. (2018). Permuco: Permutation Tests for Regression, (Repeated Measures) ANOVA/ANCOVA and Comparison of Signals [R package version 1.1.0].
- Gramfort, A., Luessi, M., Larson, E., Engemann, D. A., Strohmeier, D., Brodbeck, C., Parkkonen, L., & Hämäläinen, M. S. (2014). MNE Software for Processing MEG and EEG Data. *NeuroImage*, 86, 446–460. <https://doi.org/10.1016/j.neuroimage.2013.10.027>
- Groppe, D. M., Urbach, T. P., & Kutas, M. (2011). Mass Univariate Analysis of Event-Related Brain Potentials/Fields I: A Critical Tutorial Review. *Psychophysiology*, 48(12), 1711–1725. <https://doi.org/10.1111/j.1469-8986.2011.01273.x>
- Hester, J., Csárdi, G., Wickham, H., Chang, W., Morgan, M., & Tenenbaum, D. (2020). *Remotes: R Package Installation from Remote Repositories, Including 'GitHub'* [R package version 2.2.0]. <https://CRAN.R-project.org/package=remotes>
- Hochmann, J.-R., & Papeo, L. (2014). The Invariance Problem in Infancy: A Pupillometry Study. *Psychological Science*, 25(11), 2038–2046. <https://doi.org/10.1177/0956797614547918>
- Holm, S. (1979). A Simple Sequentially Rejective Multiple Test Procedure. *Scandinavian Journal of Statistics*, 6(2), 65–70.
- Kherad-Pajouh, S., & Renaud, O. (2010). An Exact Permutation Method for Testing any Effect in Balanced and Unbalanced Fixed Effect ANOVA. *Computational Statistics & Data Analysis*, 54(7), 1881–1893. <https://doi.org/10.1016/j.csda.2010.02.015>
- Kherad-Pajouh, S., & Renaud, O. (2015). A General Permutation Approach for Analyzing Repeated Measures ANOVA and Mixed-Model Designs. *Statistical Papers*, 56(4), 947–967. <https://doi.org/10.1007/s00362-014-0617-3>
- Luo, W.-L., & Nichols, T. E. (2003). Diagnosis and Exploration of Massively Univariate Neuroimaging Models. *NeuroImage*, 19(3), 1014–1032.
- Maris, E., & Oostenveld, R. (2007). Nonparametric Statistical Testing of EEG- and MEG-Data. *Journal of Neuroscience Methods*, 164(1), 177–190. <https://doi.org/10.1016/j.jneumeth.2007.03.024>
- Pedersen, T. L. (2020). *Patchwork: The Composer of Plots* [R package version 1.0.1]. <https://CRAN.R-project.org/package=patchwork>
- Pernet, C., Latinus, M., Nichols, T., & Rousselet, G. (2015). Cluster-Based Computational Methods for Mass Univariate Analyses of Event-Related Brain Potentials/Fields: A Simulation Study. *Journal of Neuroscience Methods*, 250, 85–93. <https://doi.org/10.1016/j.jneumeth.2014.08.003>
- Sassenhagen, J., & Draschkow, D. (2019). Cluster-Based Permutation Tests of MEG/EEG Data do not Establish Significance of Effect Latency or Location. *Psychophysiology*, 56(6), 1–8. <https://doi.org/10.1111/psyp.13335>

- Slowikowski, K. (2020). *Ggrepel: Automatically Position Non-Overlapping Text Labels with 'ggplot2'* [R package version 0.9.0]. <https://CRAN.R-project.org/package=ggrepel>
- Smith, S., & Nichols, T. (2009). Threshold-free cluster enhancement: Addressing problems of smoothing, threshold dependence and localisation in cluster inference. *NeuroImage*, 44(1), 83–98. <https://doi.org/10.1016/j.neuroimage.2008.03.061>
- Tipura, E., Renaud, O., & Pegna, A. J. (2019). Attention Shifting and Subliminal Cueing under High Attentional Load: An EEG Study Using Emotional Faces. *Neuroreport*. <https://doi.org/10.1097/WNR.0000000000001349>
- Troendle, J. F. (1995). A Stepwise Resampling Method of Multiple Hypothesis Testing. *Journal of the American Statistical Association*, 90(429), 370–378. <https://doi.org/10.1080/01621459.1995.10476522>
- Westfall, P. H., & Young, S. S. (1993). *Resampling-Based Multiple Testing: Examples and Methods for p-Value Adjustment* (1 edition). John Wiley & Sons.
- Wickham, H. (2016). *Ggplot2: Elegant Graphics for Data Analysis*. Springer-Verlag. <https://ggplot2.tidyverse.org>
- Winkler, A. M., Ridgway, G. R., Webster, M. A., Smith, S. M., & Nichols, T. E. (2014). Permutation Inference for the General Linear Model. *NeuroImage*, 92, 381–397. <https://doi.org/10.1016/j.neuroimage.2014.01.060>

A Additional Simulation Results

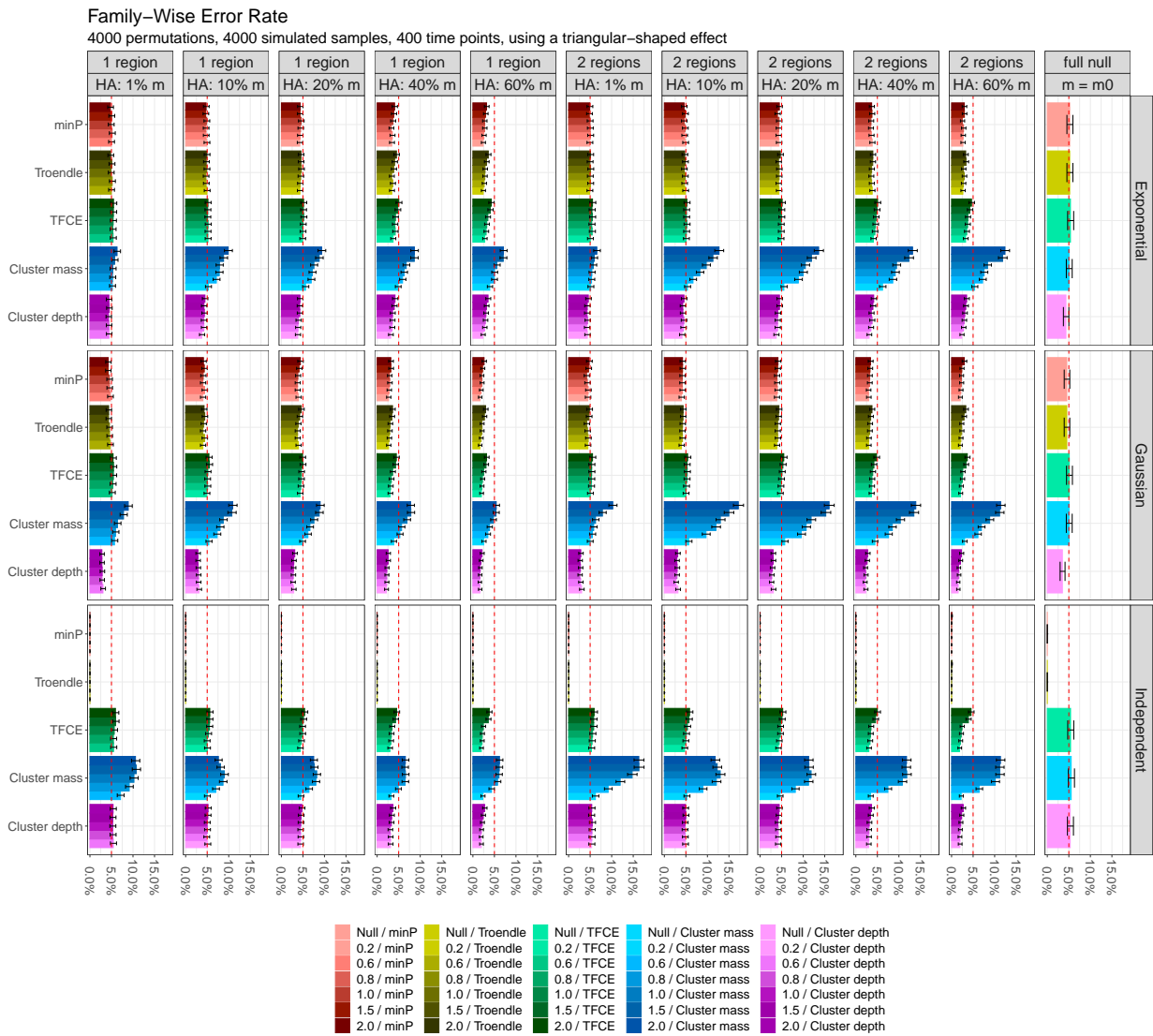


Figure A.1: Empirical FWER in the same settings as in Figure 3, except with a triangular-shaped effect, to evaluate the influence of a continuously growing effect on the FWER.

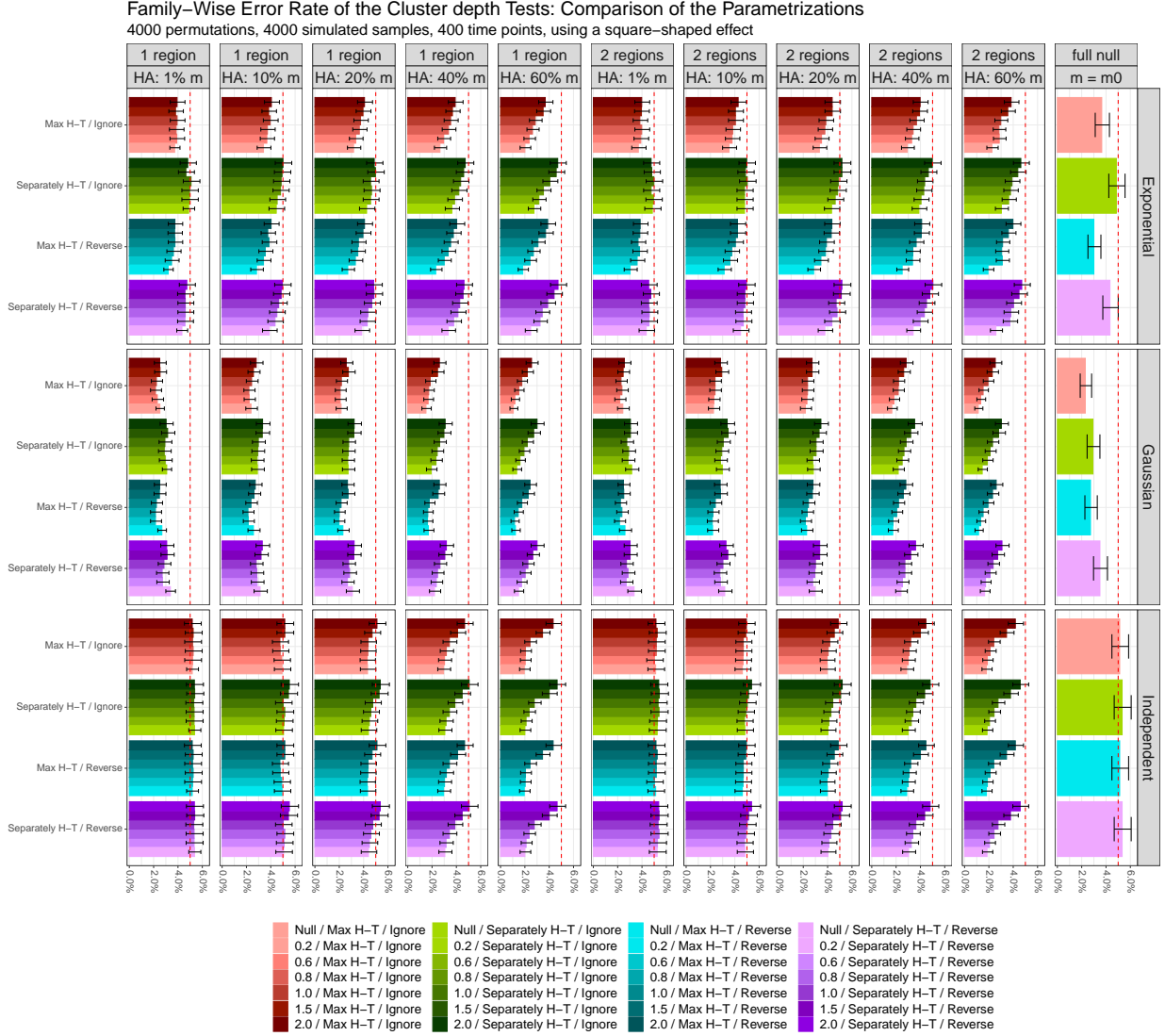


Figure A.2: Empirical FWER of the cluster depth tests for different parametrizations presented in Section 5 with 95% CI using Agresti and Coull, 1998. Different numbers and lengths of true effect regions are presented in columns, different noise structures in rows, the different parametrizations in colors, and the different effect sizes of the true effects in color luminance. The distributions of the j th cluster depth are computed either separately from the head and the tail (“Separately H-T”) or using unique distribution of the maximum over the head and tail (“Max H-T”). In addition, the cluster depth of permuted clusters at the border are computed either by reversing the clusters (“Reverse”) or by keeping unchanged the clusters within the time frame (“Ignore”). As expected, using the distributions “Max H-T” leads to slightly more conservative tests. The method to handle the clusters at the border (“Reverse” or “Ignore”) does not seem to have a systematic effect on the p -values.

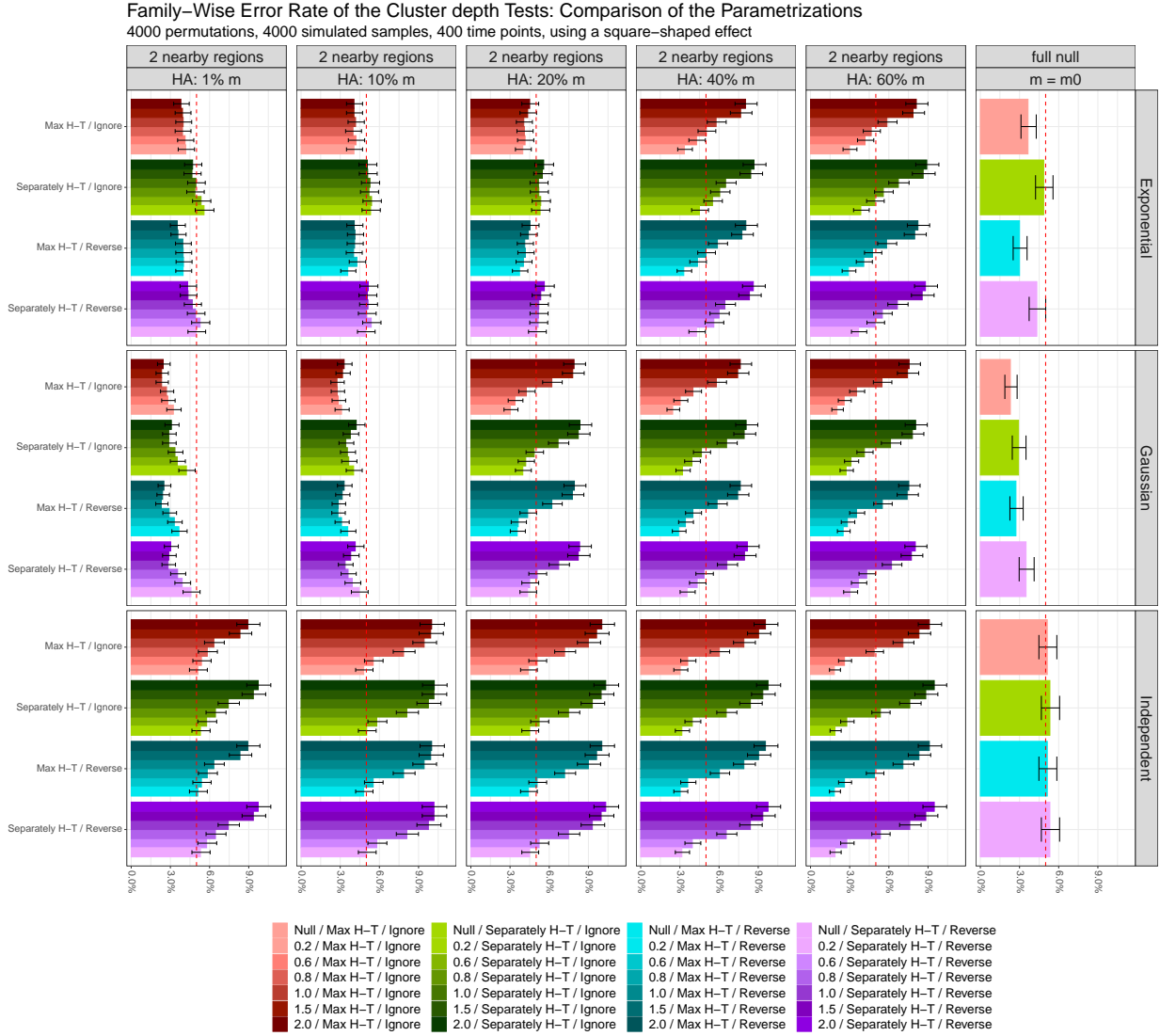


Figure A.4: Empirical FWER of the cluster depth tests under different parametrizations, similar to Figure A.2, except when the two regions of true effect are separated only by one time point under the null, as in Figure 5. It corresponds to physiologically implausible nearby regions of effect where the cluster depth tests procedure is expected to fail.

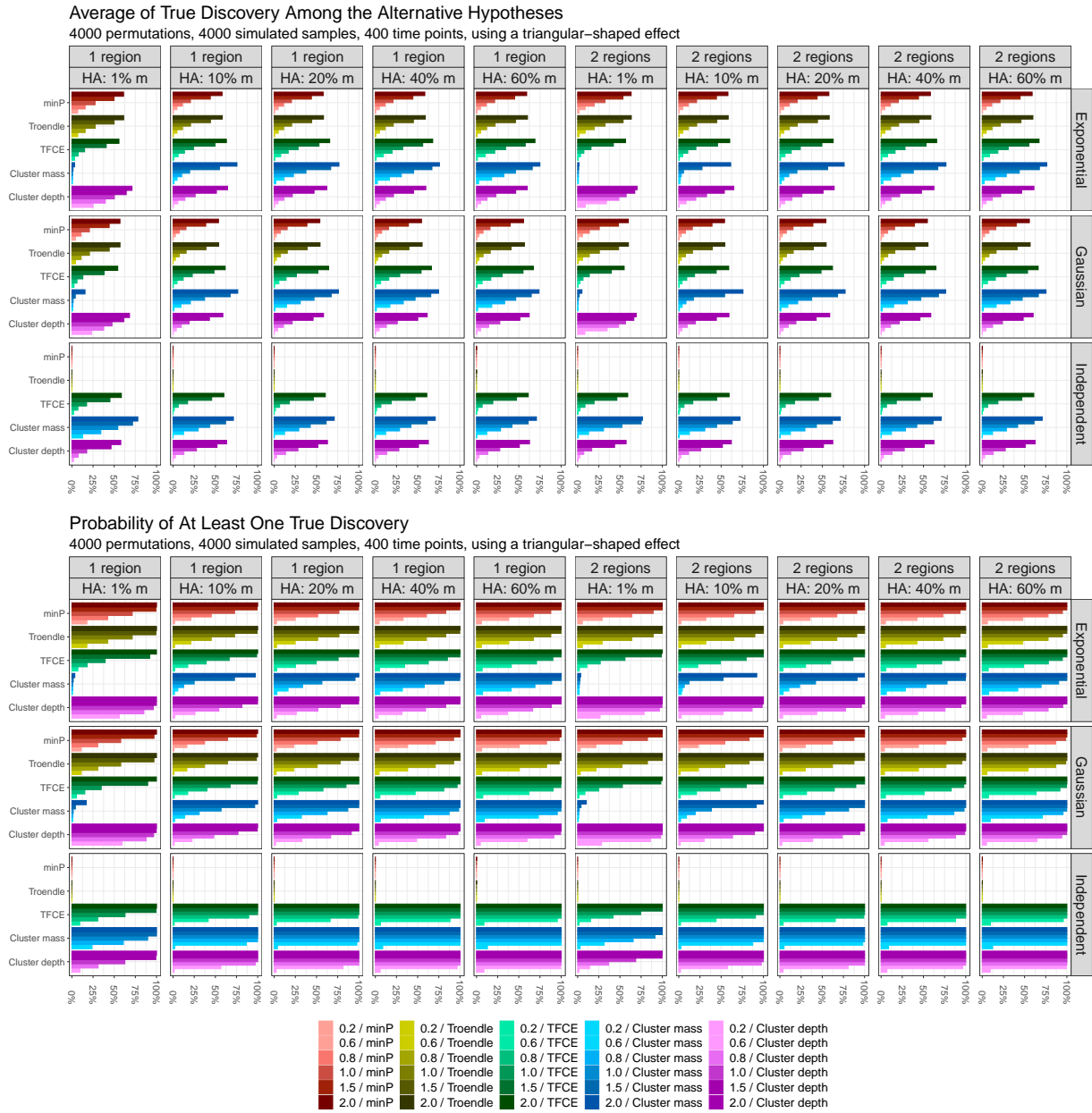


Figure A.5: Average and disjunctive power for the similarly to 4, except for a triangular-shaped effect.